Clays and Clay Minerals, Vol. 53, No. 1, 100–107, 2005.

TITANITE LOW-TEMPERATURE ALTERATION AND Ti MOBILITY

DAVID B. TILLEY† AND RICHARD A. EGGLETON*

Cooperative Research Centre for Landscape Evolution and Mineral Exploration, Department of Geology, Australian National University, Canberra, ACT 0200, Australia

Abstract—A pseudomorphous aggregate after titanite composed of smectite, anatase and residual titanite of composition $(Ca_{0.98},Mn_{0.02})(Ti_{0.65},Al_{0.35})[SiO_4](O_{0.65},OH_{0.35})$, from a depth of 450 m in the Broken Hill South Mine, New South Wales, Australia, was investigated by electron microscopy and microanalysis to characterize the alteration products and the mobility of Ti. Examination of the pseudomorph showed randomly oriented anatase crystals dispersed throughout a matrix of beidellite, with 9% porosity. Around the periphery and along the (110) cleavage plane of titanite, alteration was most developed. The range of Ti mobility was found to be limited to ~500 nm, and the ratio between the average diameter of anatase crystals and the average distance between them is ~1.3. This ratio is consistent with an alteration process in which Ti is conserved and the anatase crystals grow from the Ti available immediately around them. It is unlikely that Ti migrated beyond the titanite pseudomorph.

Key Words—Aluminous Titanite, Anatase, Beidellite, Montmorillonite, Smectite, Sphene, Titanium Mobility.

INTRODUCTION

Because of its extremely low solubility, there is little detailed information on the behavior of Ti during weathering. Many studies have concluded, or assumed, that Ti is an immobile element under supergene alteration, so much so that it is usually taken as an immobile reference element in studies of element mobility (Nesbitt, 1979; Eggleton *et al.* 1987; Middleburg *et al.*, 1988; Law *et al.*, 1991). Solubility data also suggest low mobility for Ti. According to Van Baalen (1993), Ti solubility at typical groundwater pH is so low that measurement is extremely difficult. Van Baalen's (1993) collected observations hint at a U- or V-shaped hydrolysis diagram, with total dissolved Ti at pH 3 of the order of 50 μg/L, falling below 0.01 μg/L at pH 7, then increasing to ~50 μg/L at pH 11. Only under hydrothermal alteration or during metamorphism has meter or greater scale Ti movement been clearly documented (Rubin *et al.* 1993; Van Baalen, 1993) and in particular, high CO_2 levels have been found to promote Ti solubility (Hynes, 1980; Myhra *et al.*, 1984).

In hydrothermal experiments, Matthews (1976) found that anatase was the first crystalline phase to form from amorphous TiO_2 in alkaline, neutral or mildly acid solutions at 300ºC, with later conversion to rutile.

Despite its low solubility, Ti is released from silicates as they weather, and is apparently precipitated as anatase, for this is the dominant Ti oxide of the weathering profile (Banfield *et al.*, 1993). Mitchell (1964) reported anatase pseudomorphs after sphene in the weathered part of a pegmatite from Virginia, USA, and Vance and Doern (1989) further described this and another highly porous anatase resulting from the pseudomorphous leaching of titanite by groundwater. Nesbitt *et al.* (1981) stated that titanite is stable relative to TiO_2 in groundwater with a high Ca/H ratio. Titanite leaching experiments (Metson *et al.*, 1982) with deionized water showed the development of a Ti-enriched and Ca- and Si-depleted layer, and similar experiments with glass of titanite composition showed the development of anatase on the surface. However, where Ca was present in the leaching solution, the titanite gained weight, in agreement with the thermodynamic predictions. Braun *et al.* (1993) concluded that Ti had some mobility in the weathered syenite they studied because of the presence of Ti-enriched cerianite in white clay seams, but they did not indicate the chemical conditions of its migration. Malengreau *et al.* (1995) found spectroscopic evidence for aged hydrous titania gels in sedimentary kaolinites, suggesting local mobility of Ti as colloidal hydrated Ti oxides. Clear evidence for Ti mobility at acid pH (4.5) in a ferralsol has been reported by Cornu *et al.* (1999) who, in a controlled experiment in a soil profile, reported the precipitation of anatase crystals up to 0.4 μm in diameter over an 18 month period. They concluded "Ti may be mobile at centimetric scale as well as profile scale. It moves as a dissolved element or as organo-metallic compounds."

Titanite (sphene) is classified as a monosilicate mineral (Liebau, 1982) with a major element chemical composition of $Ca(Ti >> Al,Fe^{3+})(O >> OH,F)[SiO_4]$. Substitution of Ti by Al and/or Fe is common in titanite,

* E-mail address of corresponding author:
tony.eggleton@anu.edu.au
† Present address: PO Box 1605, Queanbeyan, NSW 2620, Australia
DOI: 10.1346/CCMN.2005.0530110

Copyright © 2005, The Clay Minerals Society

https://doi.org/10.1346/CCMN.2005.0530110 Published online by Cambridge University Press

where total Al+Fe does not (normally) exceed 30 mole % and Al usually predominates over Fe (Higgins and Ribbe, 1976). In this paper we investigate the alteration of an aluminous titanite crystalline aggregate to explore the process of Ti release and to quantify the extent of its mobility under presumed supergene alteration at near neutral pH.

MATERIALS AND METHODS

The sample studied was an aggregate of 1–10 mm-sized titanite crystals in a quartz-spessartine-sphalerite rock from a depth of 450 m in the #7 Shaft of the Broken Hill South Mine, New South Wales, Australia. The titanite was partly altered to a cream colored pseudomorph of clay. The silver-lead-zinc ore deposit at Broken Hill is associated with the Early to Middle Proterozoic metamorphic rocks of the Willyama Supergroup (Willis *et al.*, 1983). At least four phases of deformation with accompanying high- to low-grade regional metamorphism have affected the rocks of the Willyama Supergroup. Minerals within the ore deposit at Broken Hill were subjected to a long and complex history of weathering and erosion (van der Heyden and Edgecombe, 1990). Oxidation and erosion peaked during the Permian while a period of less intense weathering occurred in the Cainozoic (Stevens, 1986).

A sample of titanite and altered material was removed from the specimen using a dental drill. The sample was ground to a fine powder and then dispersed onto a low-background holder cut from a single quartz crystal oriented not to Bragg-diffract X-rays. The X-ray diffraction (XRD) patterns were recorded with a Siemens D501, θ-2θ powder diffractometer using CuKα radiation and a graphite post-sample monochromator, collimated by 1° divergence slits. Quantification and cell-parameter refinement of the constituent minerals were performed using SIROQUANT, a Rietveld-type quantitative phase-analysis program (Taylor and Clapp, 1992).

Clay was separated from the powdered sample by sedimentation of the coarser fraction through a water column. The supernatant liquid containing suspended clay was pipetted onto a low-background holder and low-angle XRD patterns obtained from the air-dried clay fraction after treatment with ethylene glycol and after heating to 315°C.

Thin-sections and broken fragments of the titanite-bearing rock were examined optically and by using a JEOL 6400 and a Cambridge S360 scanning electron microscope, operating between 15 and 20 kV. Ion-beam thinned specimens were examined with a JEOL 200CX and a Philips EM430 transmission electron microscope, operating at 200 and 300 kV, respectively. Chemical analyses of the separate mineral phases were performed using energy dispersive X-ray analysis (EDXA) with the JEOL 6400 and the Philips EM430.

RESULTS

Thin-section examination of the sample revealed large (up to 10 mm) zoned and altered titanite crystals in rock composed of anhedral quartz, euhedral garnet and interstitial sphalerite. The titanite alteration appears to follow crystallographic directions.

An XRD pattern of the altered material is shown in Figure 1. All the peaks can be ascribed to titanite, smectite or anatase. Ethylene glycol treatment of the separated clay resulted in a shift of the 001 smectite peak from a *d* value of 15.2 to 17.2 Å. Heating the sample

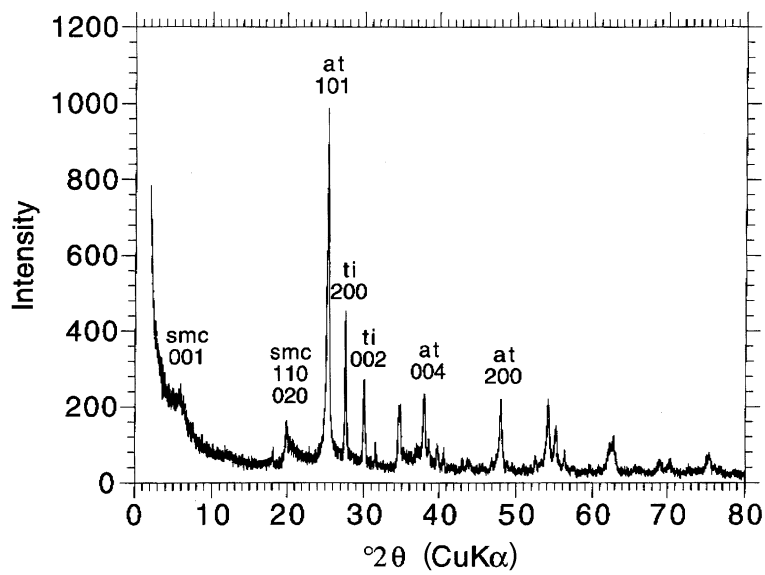


Figure 1. XRD scan of partially altered material showing peaks attributed to titanite (ti), smectite (smc) and anatase (at). For clarity, only a few peaks are labeled.

https://doi.org/10.1346/CCMN.2005.0530110 Published online by Cambridge University Press

caused a change in this d value to 10.4 Å and a significant reduction in the peak's intensity (Figure 2).

The mineralogical composition of the partially altered material, as determined by SIROQUANT is 23 wt.% titanite, 30 wt.% anatase and 47 wt.% smectite. Recalculation of the analysis to exclude titanite gives a composition of 39 wt.% anatase and 61 wt.% smectite. Cell-parameter refinement of the aluminous titanite yielded the following values: a = 7.047 Å, b = 8.656 Å, c = 6.533 Å and β = 114.21°. The unit-cell dimensions of the anatase are a, b = 3.787 Å and c = 9.488 Å and those of the smectite are approximately a = 5.2 Å, b = 9.1 Å and d_{001} = 15.2 Å.

Back-scattered electron images of an altered titanite crystal display smooth mid-gray regions composed of titanite having a strong linear configuration interpreted as titanite's (110) cleavage plane (Figure 3a). The intervening zones have a rough terrain consisting of an intimate mixture of anatase (bright) and smectite (dark). Polished sections of the altered titanite show marked atomic number contrast between anatase and smectite, and allow quantification of the area occupied by anatase in the pseudomorph (Figure 4). Eight areas yielded an average of 26% anatase (range 36–16%, S.D. = 7%)

Secondary electron microscopy revealed varying degrees of alteration (Figure 3b-d). The smooth, elongate regions of Figure 3b are titanite while the regions between are a mixture of smectite and anatase. In general, a sharp boundary exists between fresh titanite and altered material. The smectite has a typical web-like morphology and is closely associated with well-formed

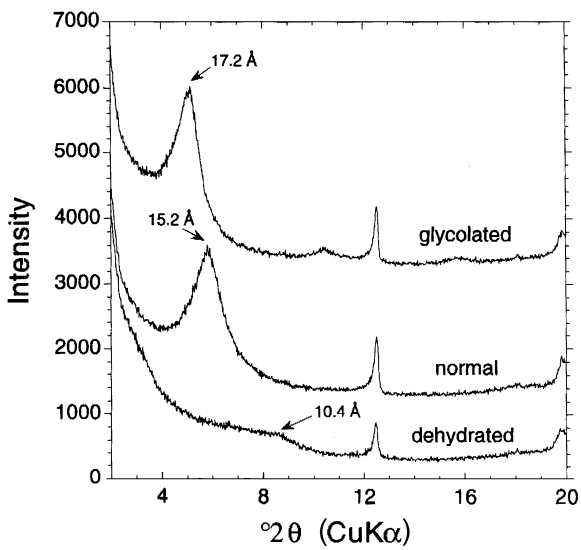


Figure 2. XRD scan of the altered material before and after ethylene glycol treatment. A shift in the 001 peak of smectite from a d value of 15.5 Å to 16.9 Å occurred as a result of the treatment. Dehydration at 315°C resulted in the collapse of the interlayer spacing causing a shift in the 001 smectite peak to 10.4 Å.

Table 1. Average diameter of anatase crystals and the number per 100 μm^2.

Diameter (μm)	Crystals/ 100 μm^2
0.7	46.6
1.1	18.7
1.3	11.3
1.4	13.4
1.5	8.3
1.6	9.4

bipyramidal anatase crystals which are randomly distributed and randomly oriented (Figure 3c,d). The faces of the anatase crystals are noticeably curved. The size and separation of anatase crystals were assessed by counting the number of these on different micrographs and measuring their mean diameter (Table 1).

Transmission electron microscopy (TEM) of the partially altered material revealed web-like smectite surrounding elongate regions of relatively unaltered titanite. Embedded within the smectite are grains of anatase. Closer examination revealed the boundary between the altered material and titanite to be pitted, suggestive of a chemical etching process (Figure 5). A close association between anatase and smectite was commonly observed with TEM. Around the periphery of anatase grains, smectite envelops and is intergrown with the anatase (Figure 6). In areas where anatase crystal morphology is not as well developed, this intimate relationship is even more apparent (Figure 7). Selected area electron diffraction (SAED) patterns of such areas displayed arcs rather than spots associated with anatase, indicating that the anatase crystals are randomly oriented (Figure 7, inset). The SAED of the smectite was difficult to obtain because of damage from the ion beam during thinning and from the TEM's electron beam; however, faint rings were occasionally observed suggesting a random orientation for the smectite.

The EDXA results for titanite, smectite and anatase are given in Tables 2, 3 and 4. The titanite contains 10.0 wt.% Al_2O_3 and has a structural formula calculated on the basis of one Si atom: $(Ca_{0.98},Mn_{0.02})(Ti_{0.65},Al_{0.35})[SiO_4](O_{0.65},OH_{0.35})$. The structural formula of the smectite, calculated on a basis of $O_{20}(OH)_4$ and assuming that the Ti reported in the smectite analysis

Table 2. Chemical analyses (wt.%) by EDXA of titanite.

	1	2	3	4	5	Average
SiO_2	32.3	31.8	31.6	31.6	32.0	31.9
TiO_2	28.2	27.8	27.8	29.0	28.6	28.3
Al_2O_3	10.6	10.1	10.0	9.4	9.9	10.0
MnO	0.8	0.9	0.8	0.6	0.7	0.8
CaO	30.0	29.0	29.0	29.2	29.4	29.3
Total						100.3

https://doi.org/10.1346/CCMN.2005.0530110 Published online by Cambridge University Press

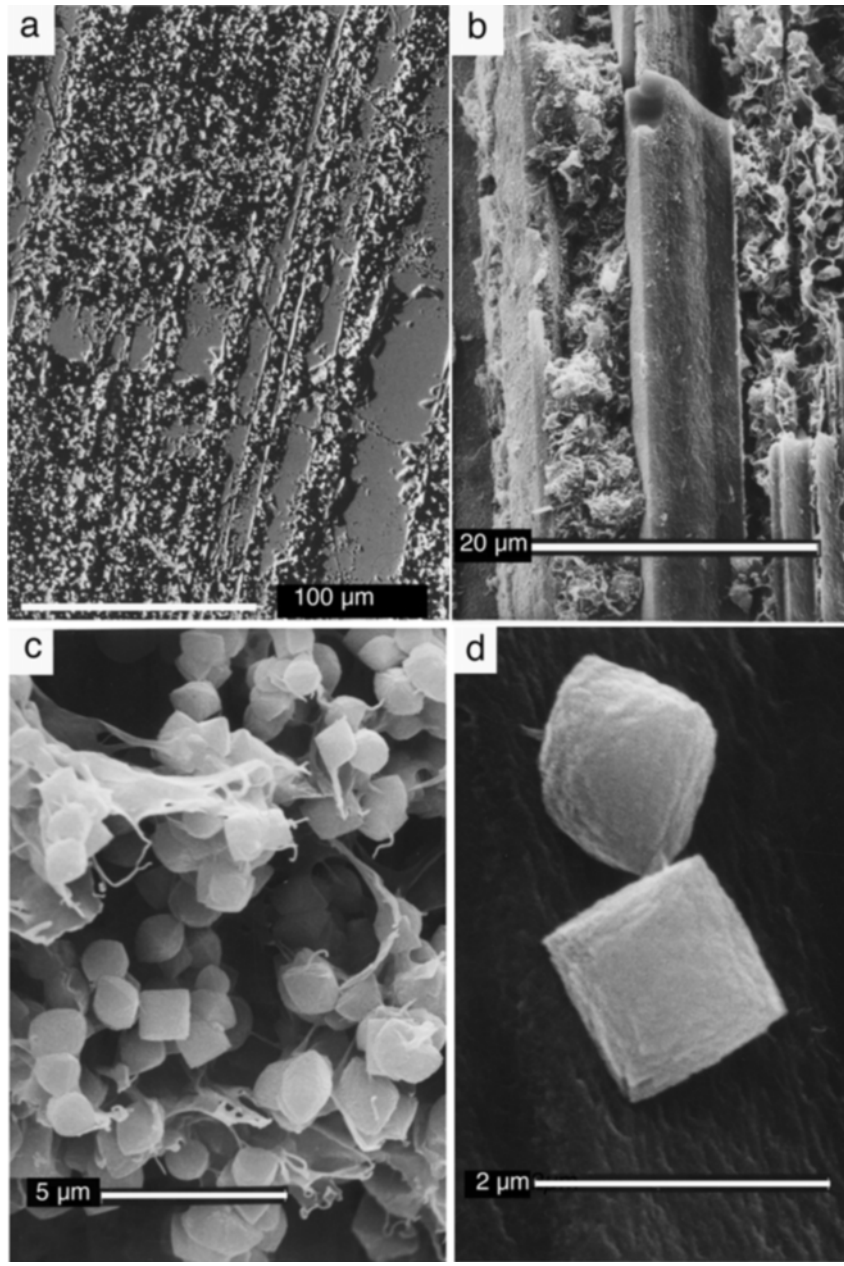


Figure 3. (a) BSE image of a thin-sectioned altered titanite crystal showing a strong linear configuration of minerals coincident with the (110) cleavage plane of titanite. The rough terrain shows an intimate mixture of anatase (bright) and smectite (dark). The smooth mid-gray regions are titanite. Scale bar = 100 µm. (b) Secondary electron micrograph of the cleaved surface of an altered titanite crystal. The smooth, elongate regions are titanite while the intervening zones contain a mixture of smectite and anatase. Scale bar = 20 µm. (c) Secondary electron micrograph of smectite with a typical web-like morphology and closely associated bipyramidal anatase crystals. Scale bar = 5 µm. (d) Secondary electron micrograph of anatase crystals displaying a bipyramidal form with slightly spheroidal faces. Scale bar = 2 µm.

is from included anatase, is $(Ca_{0.12}Na_{0.31}K_{0.07})^{0.62+}$ $(Al_{3.46}Fe_{0.20}Mg_{0.49})(Si_{7.42}Al_{0.58})O_{20}(OH)_4$. The chemical analysis of the smectite is indicative of beidellite, as the layer charge arises in the tetrahedral sheet.

Individual anatase grains could not have their chemistry confidently determined, even with EDXA, due to their small grain size and possible contamination with the intergrown smectite. Analysis of the anatase grains gave a composition of ~90 wt.% TiO_2 together with 1 wt.% Al_2O_3, 6 wt.% SiO_2, 2 wt.% CaO and 2 wt.% FeO. Selected (highest Ti) analyses in Table 3 show the range of compositions obtained.

https://doi.org/10.1346/CCMN.2005.0530110 Published online by Cambridge University Press

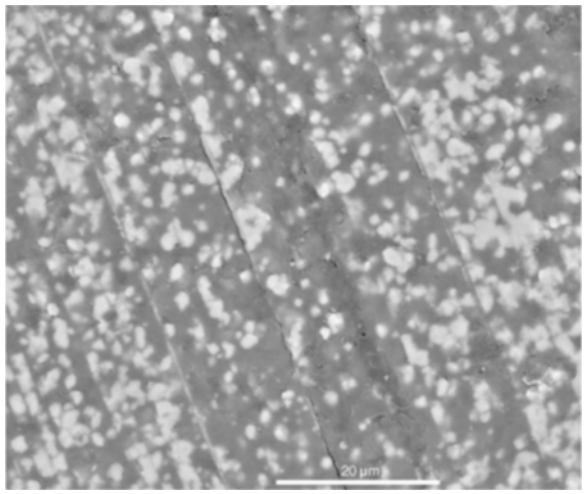


Figure 4. BSE image of a polished section of titanite alteration. Anatase crystals are bright.

DISCUSSION

Synthetic titanite with the formula $CaTi(SiO_4)O$ has unit-cell parameters of a = 7.069, b = 8.722, c = 6.566 and β = 113.86° (Speer and Gibbs, 1976). The aluminous titanite presented here has a smaller unit-cell, due to Al substituting for Ti (Ribbe, 1982). Although high, 10.0 wt.% Al_2O_3 substitution in the titanite is not the maximum attainable. An aluminous titanite investigated by Franz and Spear (1985) was found to contain as much as 14.1 wt.% Al_2O_3, corresponding to the theoretical limit of 0.5 mole per structural formula.

In hand specimen and by optical microscopy, the aluminous titanite appears to have altered isovolumetrically, as no expansive or contractive features are evident in or around the altered crystal. To determine if this was indeed the case, the volume occupied by titanite, smectite and anatase was calculated. One unit-cell of titanite has a volume of 363.5 Å^3, of smectite 719.3 Å^3 and of anatase 136.1 Å^3. A simplified equation for the alteration of aluminous titanite assuming Ti constant may be written as:

$$12Ca(Ti_{0.67}Al_{0.33})(SiO_4)O_{0.67}OH_{0.33} + 4H_2O + 0.7(Fe,Mg)O \rightarrow (Al_{3.5}(Fe,Mg)_{0.7})(Si_{7.5}Al_{0.5})O_{20}(OH)_4Ca_{0.25}.4H_2O + 8TiO_2 + 4.5SiO_2 + 11.75CaO$$

Both titanite and anatase contain four structural units per unit-cell, whereas smectite has one (Deer *et al*,. 1992). At constant Ti, the equation requires that 12 moles of titanite (1090.5 Å^3) alter to 1 mole of smectite (719.3 Å^3) and 8 moles of anatase (272.2 Å^3), which would result in the production of 9% porosity. Using the simplified equation above and densities of 2.27 g cm^{-3} for smectite and 3.90 g cm^{-3} for anatase, the alteration product would be composed of 61 wt.% smectite and 39 wt.% anatase, which is the same composition as determined by SIROQUANT. The reaction as proposed is conservative of Al as well as the assumed Ti conservation.

The size, degree of euhedral development and the distance between adjacent anatase grains appear to be

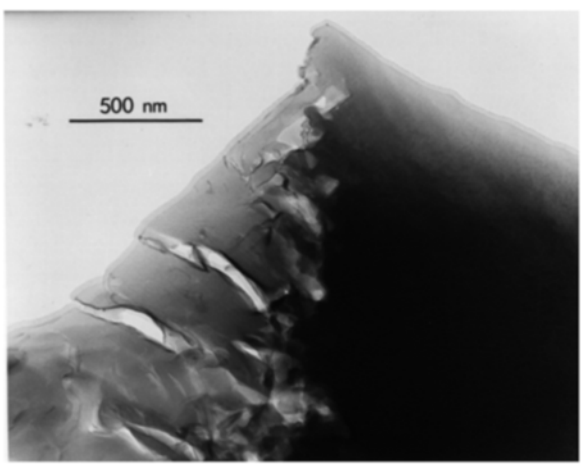


Figure 5. TEM image of the boundary between titanite and the altered material. The featureless material on the right of the micrograph is titanite while the relatively porous material on the left is smectite. Scale bar = 500 nm.

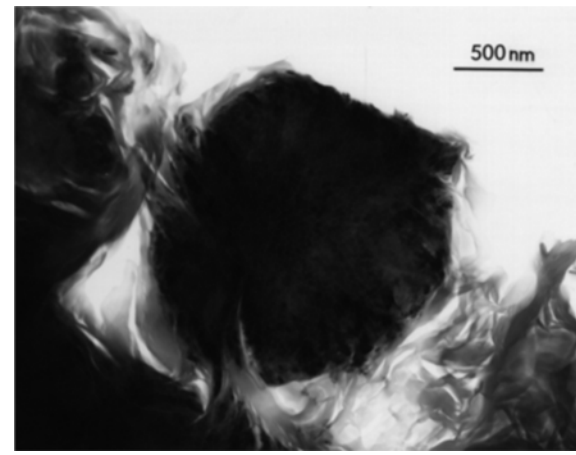


Figure 6. TEM image of an anatase grain. Around the edge of the grain, smectite envelops and intergrows with the anatase. Scale bar = 500 nm.

Table 3. Chemical analyses (wt.%) by EDXA of smectite.

	1	2	3	4	Average
SiO_2	60.4	59.8	57.7	58.8	59.2
TiO_2	0.7	0.8	1.3	0.5	0.8
Al_2O_3	26.5	27.3	27.3	28.6	27.4
FeO	2.0	2.2	2.0	2.0	2.1
MgO	2.9	2.7	2.3	2.3	2.6
CaO	0.9	0.9	0.8	0.8	0.9
Na_2O	1.3	1.4	1.1	1.3	1.3
K_2O	0.4	0.5	0.3	0.3	0.4
Total					94.7

https://doi.org/10.1346/CCMN.2005.0530110 Published online by Cambridge University Press

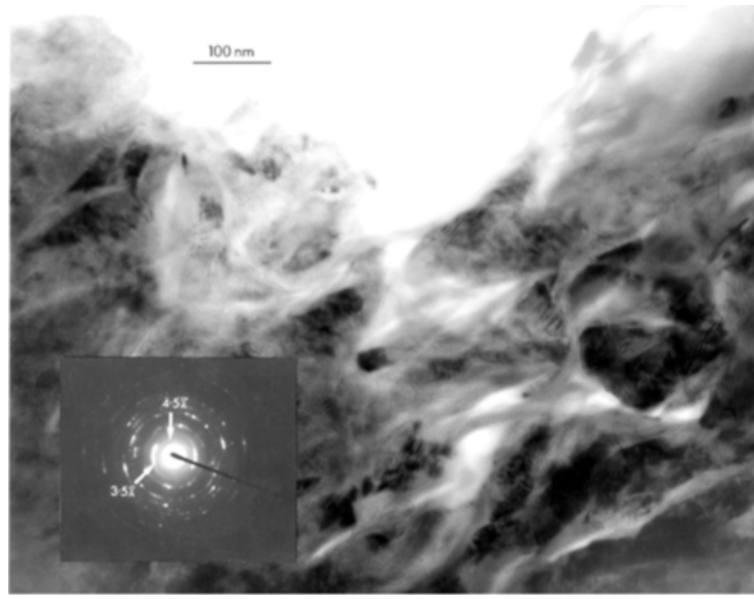


Figure 7. TEM image of small, poorly formed anatase crystals intimately associated with smectite. The SAED pattern (inset) displays arcs of 3.5 and 4.5 Å attributed to diffraction from the (101) plane of anatase and the (100) plane of smectite, respectively. The arcs are indicative of diffraction from crystals not having the same orientation.

intrinsically related to the degree of Ti mobility and migration. From TEM images, well-formed anatase crystals of 1200 nm diameter were measured to have an average spacing of 900 nm between grains, while poorly formed crystals of 72 nm diameter were, on average, 54 nm apart. From SEM images, an inverse relationship between anatase crystal size and mean separation was also found (Table 1). This relationship suggests that the anatase crystals formed only from the Ti in their immediate surrounds, with more abundant nuclei being limited in their opportunity to grow compared to regions of fewer anatase nuclei. In either case, if the Ti is locally derived, the proportion of anatase should be the same; 38% by weight as calculated above, or 27% by volume. The measured value of 26 volume % for anatase is in agreement with this interpretation. On this basis, an anatase crystal sweeps up Ti from a shell of radius twice that of the crystal. Consequently, the maximum average distance found for the migration of Ti is of the order of 600 nm (the radius of the largest crystals). Despite these general trends, there is considerable local variation in anatase crystal concentration (*e.g.* Figure 3c which shows an unusually high concentration of anatase crystals). The crystals themselves may well have moved after crystallization, or the Ti diffusion through the altering titanite may have been irregular. In no case, however, is there evidence of greater than micron-scale movement of Ti.

The complete randomness in the orientation of the anatase grains relative to the original titanite crystals suggests the mechanism for titanite's alteration to be a dissolution-precipitation process rather than one of solid-state transformation. The environment of alteration of this titanite can be interpreted from the mineral assemblage of beidellite, anatase, quartz, spessartine and sphalerite and knowledge of the Broken Hill deposit. According to King and O'Driscoll (1953) and Plimer (1984), supergene alteration at Broken Hill is pervasive to a depth of ~100 m, with leached channels reported to 600 m and deeper. There is little available data on the chemistry of the mine waters; however, the pH of waters coming from the old South Mine workings ranged from

Table 4. Chemical analyses (wt.%) by EDXA of anatase.

	1	2	3	4	5	6	7	8	Average
SiO_2	6.0	7.1	4.8	4.6	6.5	6.1	4.8	6.5	5.8
TiO_2	88.7	87.2	90.1	90.6	88.8	90.2	91.9	89.9	89.7
Al_2O_3	1.2	1.6	0.8	0.7	2.1	1.2	1.0	1.5	1.3
FeO	1.3	1.4	1.4	1.3	1.7	1.7	1.3	1.5	1.5
CaO	2.8	2.7	2.9	2.8	0.9	0.8	0.9	0.6	1.8
Total									100.1

https://doi.org/10.1346/CCMN.2005.0530110 Published online by Cambridge University Press

6–6.5 (F. Barrett, Pasminco, pers. comm.). On the basis of the thermodynamic data presented by Nesbitt *et al.* (1981), the presence of beidellite suggests silica activity in the vicinity of 10^{-3} molar, and this in turn would require Ca activity of about one molar or more to maintain equilibrium with titanite at pH 6. Typical Ca activities for groundwater (Tardy, 1971) range up to 10^{-3} molar, and at this concentration (log $[Ca]/[H]^2 = 9$) titanite would dissolve, precipitating TiO_2. The presence of sphalerite shows the alteration environment was not oxidizing. Thus the internal evidence allows that the alteration of the Broken Hill titanite was achieved by reductive supergene processes, although it does not prove this.

CONCLUSIONS

Aluminous titanite, under probable supergene conditions at neutral pH, alters to a mixture of beidellite and anatase by complete breakdown of the titanite structure and crystallization of the weathering products. Almost all the Ca in titanite is lost. The results presented here support the assumption of Ti immobility in this environment. All the Ti originally in the titanite can be accounted for by the anatase in the pseudomorph. The distribution of anatase crystals in the pseudomorph is consistent with short migration distances of Ti, generally <1 μm.

ACKNOWLEDGMENTS

This work was supported by Grant SARC 94020 from the Australian Research Council (ARC) and through the Australian Government's Cooperative Research Centres Program. SEM was performed using the facilities of the EM unit at the Research School of Biological Sciences, ANU. Analytical TEM using the nano-probe on the Philips EM430 was undertaken at the Research School of Earth Sciences, ANU.

REFERENCES

Banfield, J.F., Bischoff, B.L. and Anderson, M.A. (1993) TiO_2 accessory minerals: coarsening, and transformation kinetics in pure and doped synthetic nanocrystalline materials. *Chemical Geology*, **110**, 211–231.

Braun, J.-J., Pagel, M., Herbillon, A. and Rosin, C. (1993) Mobilization and redistribution of REEs and thorium in a syenitic lateritic profile: A mass balance study. *Geochimica et Cosmochimica Acta*, **57**, 4419–4434.

Cornu, S., Lucas, Y., Lebonc, E., Ambrosi, J.-P., Luizão, F., Rouiller, J., Bonnay, M. and Neal, C. (1999) Evidence of titanium mobility in soil profiles, Manaus, central Amazonia. *Geoderma*, **91**, 281–295.

Deer, W.A., Howie, R.A. and Zussman, J. (1992) *An Introduction to the Rock-Forming Minerals*. Longman Scientific & Technical, Harlow, Essex, England, 696 pp.

Eggleton, R.A., Varkevisser, D. and Foudoulis, C. (1987) The weathering of basalt: changes in bulk chemistry and mineralogy. *Clays and Clay Minerals*, **35**, 161–169.

Franz, G. and Spear, F.S. (1985) Aluminous titanite (sphene) from the eclogite zone, south central Tauern Window, Austria. *Chemical Geology*, **50**, 33–46.

Higgins, J.B. and Ribbe, P.H. (1976) The crystal chemistry and space groups of natural and synthetic titanites. *American Mineralogist*, **61**, 878–888.

Hynes, A. (1980) Carbonatization and Mobility of Ti, Y, and Zr in Ascot Formation Metabasalts, SE Quebec. *Contributions to Mineralogy and Petrology*, **75**, 79–87.

King, H.F. and O'Driscoll, E.S. (1953) The Broken Hill Lode. Pp. 578–600 in: *Geology of Australian Ore Deposits* (A.B. Edwards, editor). 5th Empire Mining and Metallurgical Congress, Melbourne.

Law, K.R., Nesbitt, H.W. and Longstaffe, F.J. (1991) Weathering of granitic tills and the genesis of a podzol. *American Journal of Science*, **291**, 940–955.

Liebau, F. (1982) Classification of silicates. Pp. 1–24 in: *Orthosilicates* (P.H. Ribbe, editor). Reviews in Mineralogy, **5**. Mineralogical Society of America, Washington, D.C.

Malengreau, N., Muller, J.-P. and Calas, G. (1995) Spectroscopic approach for investigating the status of Ti in kaolinitic materials. *Clays and Clay Minerals*, **43**, 621.

Matthews, A. (1976) The crystallization of anatase and rutile from amorphous titanium dioxide under hydrothermal conditions. *American Mineralogist*, **61**, 419–424.

Metson, J.B., Bancroft, G.M., Kanetkar, S.M., Nesbitt, H.W., Fyfe, W.S. and Hayward, P.J. (1982) Leaching of natural and synthetic sphene and perovskite. Pp. 329–338 in: *Scientific Basis for Nuclear Waste Management V* (W. Lutze, editor). Materials Research Society Symposia Proceedings, **11**.

Middleburg, J.J., Van der Weijden, C.H. and Woittiez, J.R.W. (1988) Chemical processes affecting the mobility of major, minor and trace elements during weathering of granitic rocks. *Chemical Geology*, **68**, 253–273.

Mitchell, R.S. (1964) Pseudomorphs of anatase after sphene from Roanoke County, Virginia. *American Mineralogist*, **49**, 1136–1139.

Myhra, S., Savage, D., Atkinson, A. and Rivière, J.C. (1984) Surface modification of some titanite minerals subjected to hydrothermal chemical attack. *American Mineralogist*, **69**, 902–909.

Nesbitt, H.W. (1979) Mobility and fractionation of rare earth elements during weathering of granodiorite. *Nature*, **279**, 206–210.

Nesbitt, H.W., Bancroft, G.M., Karkhanis, S.N. and Fyfe, W.S. (1981) The stability of perovskite and sphene in the presence of backfill and repository minerals: A general approach. Pp. 131–138 in: *Scientific Basis for Nuclear Waste Management III* (J.G. Moore, editor). Plenum, New York.

Plimer, I.R. (1984) The mineralogical history of the Broken Hill Lode, NSW. *Australian Journal of Earth Sciences*, **31**, 379–402.

Ribbe, P.H. (1982) Titanite (sphene). Pp. 137–154 in: *Orthosilicates* (P.H. Ribbe, editor). Reviews in Mineralogy, **5**. Mineralogical Society of America, Washington, D.C.

Rubin, J.N., Henry, C.D. and Price, J.G. (1993) The mobility of zirconium and other "immobile" elements during hydrothermal alteration. *Chemical Geology*, **110**, 29–47.

Speer, J.A. and Gibbs, G.V. (1976) The crystal structure of synthetic titanite, $CaTiOSiO_4$, and the domain textures of natural titanites. *American Mineralogist*, **61**, 238–247.

Stevens, B.P.J. (1986) Post-depositional history of the Willyama Supergroup in the Broken Hill Block, New South Wales. *Australian Journal of Earth Science*, **33**, 73–98.

Tardy, Y. (1971) Characterization of the principal weathering types by the geochemistry of waters from some European and African crystalline massifs. *Chemical Geology,* **7**, 253–271.

https://doi.org/10.1346/CCMN.2005.0530110 Published online by Cambridge University Press

Taylor, J.C. and Clapp, R.A. (1992) New features and advanced applications of SIROQUANT: a personal computer XRD full profile quantitative analysis software package. *Advances in X-ray Analysis*, **35**, 49–55.

van Baalen, M.R. (1993) Titanium mobility in metamorphic systems: a review. *Chemical Geology*, **110**, 233–249.

van der Heyden, A. and Edgecombe, D.R. (1990) Silver-lead-zinc deposit at South Mine, Broken Hill. Pp. 1073–1077 in: *Geology of the Mineral Deposits of Australia and Papua New Guinea* (F.E. Hughes, editor). The Australasian Institute of Mining and Metallurgy.

Vance, E.R. and Doern, D.C. (1989) The properties of anatase pseudomorphs after titanite. *The Canadian Mineralogist*, **27**, 495–498.

Willis, I.L., Brown, R.E., Stroud, W.J. and Stevens, B.P.J. (1983) The Early Proterozoic Willyama Supergroup: stratigraphic subdivision and interpretation of high to low-grade metamorphic rocks in the Broken Hill Block, New South Wales. *Journal of the Geological Society of Australia*, **30**, 195–224.

(*Received 11 November 2002; revised 5 December 2004; Ms. 737*)

https://doi.org/10.1346/CCMN.2005.0530110 Published online by Cambridge University Press